

All-electron basis sets for H to Xe specific for ZORA calculations: Applications in atoms and molecules

C. S. Gomes, F. E. Jorge, and A. Canal Neto

Citation: Chin. Phys. B, 2024, 33 (**8**): 083101. DOI: 10.1088/1674-1056/ad4bbe

What follows is a list of articles you may be interested in

All-electron ZORA triple zeta basis sets for the elements Cs-La and Hf-Rn

Antônio Canal Neto, Francisco E. Jorge, and Henrique R. C. da Cruz
Chin. Phys. B, 2023, 32 (**9**): 093101. DOI: 10.1088/1674-1056/acbe34

Spectroscopy and scattering matrices with nitrogen atom: Rydberg states and optical oscillator strengths

Yuhao Zhu(朱宇豪), Rui Jin(金锐), Yong Wu(吴勇), and Jianguo Wang(王建国)
Chin. Phys. B, 2022, 31 (**4**): 043103. DOI: 10.1088/1674-1056/ac1f05

CCSD(T) study on the structures and chemical bonds of AnO molecules (An=Bk-Lr)

Xiyuan Sun(孙希媛), Pengfei Yin(殷鹏飞), Kaiming Wang(王开明), and Gang Jiang(蒋刚)
Chin. Phys. B, 2021, 30 (**3**): 033101. DOI: 10.1088/1674-1056/abc3b1

Exploration and elaboration of photo-induced proton transfer dynamical mechanism for novel 2-[1,3]dithian-2-yl-6-(7aH-indol-2-yl)-phenol sensor

Lei Xu(许磊), Tian-Jie Zhang(张天杰), Qiao-Li Zhang(张巧丽), Da-Peng Yang(杨大鹏)
Chin. Phys. B, 2020, 29 (**5**): 053102. DOI: 10.1088/1674-1056/ab8208

Benchmarking PBE+D3 and SCAN+rVV10 methods using potential energy surfaces generated with MP2+ ΔCCSD(T) calculation

Jie Chen(陈劼), Weiyu Xie(谢炜宇), Kaihang Li(李开航), Shengbai Zhang(张绳百), Yi-Yang Sun(孙宜阳)
Chin. Phys. B, 2020, 29 (**1**): 013102. DOI: 10.1088/1674-1056/ab5fbb

---

All-electron basis sets for H to Xe specific for ZORA calculations: Applications in atoms and molecules

C. S. Gomes[1], F. E. Jorge[1,2,†], and A. Canal Neto[1]

[1] *Departamento de Física, Universidade Federal do Espírito Santo, 29075-910 Vitória, ES, Brazil*
[2] *Departamento de Física, Instituto de Ciências Exatas e Biológicas, Universidade Federal de Ouro Preto, Campus Universitário Morro do Cruzeiro, 35402-136 Ouro Preto, MG, Brazil*

(Received 17 February 2024; revised manuscript received 12 May 2024; accepted manuscript online 15 May 2024)

A segmented basis set of quadruple zeta valence quality plus polarization functions (QZP) for H through Xe was developed to be used in conjunction with the ZORA Hamiltonian. This set was augmented with diffuse functions to describe electrons farther away from the nuclei adequately. Using the ZORA-CCSD(T)/QZP-ZORA theoretical model, atomic ionization energies and bond lengths, harmonic vibrational frequencies, and atomization energies of some molecules were calculated. The addition of core-valence corrections has been shown to improve the agreement between theoretical and experimental results for molecular properties. For atomization energies, a similar observation emerges when considering spin-orbit couplings. With the augmented QZP-ZORA set, static mean dipole polarizabilities of a set of atoms were calculated and compared with previously published recommended and experimental values. Performance evaluations of the ZORA and Douglas–Kroll–Hess Hamiltonians were made for each property studied.

Keywords: QZP-ZORA and AQZP-ZORA basis sets, elements from H to Xe, CCSD(T) method, atomic and molecular properties

PACS: 31.15.ae, 31.15.aj, 31.15.ap, 31.15.eg **DOI:** 10.1088/1674-1056/ad4bbe

1. Introduction

To select a basis set to perform atomic and/or molecular calculations, two criteria such as size and precision are considered. In addition, this basis set should belong to a hierarchical sequence of sets that systematically approach the limit of the complete basis set (CBS).

Ahlrichs *et al.*[1–3] developed several contracted basis sets for the elements from H to Kr. Almlöf and Taylor[4] found that natural orbitals, generated from correlated atomic calculations, produce excellent molecular property results. Dunning *et al.*[5–8] presented the correlation-consistent polarized valence (cc-pVXZ, X = D, T, Q, 5, and 6) basis sets for the H–Ar and Ga–Kr elements. Unlike Dunning *et al.*, who used the general contraction scheme proposed by Raffenet,[9] Jorge *et al.* used Dunning's segmented contraction scheme[10] to construct basis sets of double,[11–13] triple,[14–16] and quadruple[14,17] zeta valence qualities plus polarization functions (XZP, X = D, T, and Q) for H–Xe elements. To accurately describe electrons distant from the nuclei, these latter sets were augmented with diffuse functions and then designated as AXZP.[11,18–22] What all of these sets have in common is that they describe all the electrons in the system.

Some effects are not included in conventional calculations of the electronic structures of atoms, molecules, and clusters. Among them, we cannot fail to mention relativistic effects. Certainly, the Dirac equation naturally incorporates these corrections, however, this equation gives rise to four-component wave functions, which makes their use in medium and large-sized molecules prohibitive. To reduce the computational cost, some approximations have been proposed. Among them, two of them, namely, the zero-order regular approximation (ZORA)[23] of the Dirac Hamiltonian and the Douglas–Kroll–Hess (DKH) unitary transformation, have been used extensively.[24–26] Perturbation theory is usually used to estimate spin–orbit (SO) coupling.

De Jong *et al.*[27] found that the conjunction of the DKH Hamiltonian with a non-relativistic basis set can produce undesirable results, especially for molecules containing elements from the second row of the periodic table onwards. To get around this problem, they used the DKH Hamiltonian to recontract the values of the contraction coefficients of the non-relativistic cc-pVXZ (X = D, T, Q, and 5) basis sets for H, He, B–Ne, Al–Ar, and Ga–Br. To incorporate scalar relativistic effects, Jorge *et al.* used the second-order DKH (DKH2) Hamiltonian to recontract the values of the contraction coefficients of the XZP (X = D, T, and Q) basis sets for H–Xe. These sets have been called XZP-DKH[13,16,17,28] and used by several research groups.[29–34] Other basis sets for all-electrons generated from the DKH2 or third-order DKH (DKH3) Hamiltonian have also been reported in literature. Roos *et al.*[35–37] have developed ANO basis sets for Li–Rn, which are specific for DKH2 calculations, whereas Noro *et al.* presented a hierarchical sequence of Sapporo-DKH3 basis sets for K–Xe.[38] To assess the quality of relativistic pseudopotentials, Peterson *et al.* constructed DKH basis sets of different qualities for Sc–Zn

†Corresponding author. E-mail: francisco.jorge@ufes.br

© 2024 Chinese Physical Society and IOP Publishing Ltd

and Y–Pd.[39,40]

Recently, Canal Neto *et al.*[41] showed that undesirable results can occur when using a specific basis set for DKH2 calculations together with the ZORA Hamiltonian. While the number of basis sets for all electrons specific to ZORA calculations is scarce in literature, the number of programs (DIRAC, ORCA, ADF, NWChem, etc.) that use this Hamiltonian is not. We are aware of the ZORA basis sets available in the ADF program, however, it is worth mentioning that these sets were generated from Slater-type functions, while most quantum chemistry programs can handle Gaussian-type functions (GTFs). A family of ZORA basis sets for Hf–Hg, which use GTFs, have been reported by Pantazis *et al.*[42] To include a larger number of atoms from the periodic table, Jorge *et al.* developed accurate and compact *X*ZP-ZORA (X = D and T) basis sets for H–Xe.[41,43]

To reduce the truncation error of the basis set, in this article, we decided to introduce the QZP-ZORA basis set for H–Xe. To this set, diffuse functions were added, giving rise to the AQZP-ZORA set. Using the ZORA-CCSD(T) method, the efficacy of the QZP-ZORA set was tested by calculating atomic ionization energies and bond lengths (r_e), atomization energies (D_0), and harmonic vibrational frequencies (ω_e) of a set of molecules, while that of the AQZP-ZORA set in calculating static mean dipole polarizabilities of some atoms. We also evaluated the performances of the DKH and ZORA Hamiltonians for each property studied.

2. Constructing ZORA basis sets

The procedure used to develop the QZP-ZORA basis set for elements H through *X* is similar to that in Refs. [41,43]. For each atom in the ground state, we started with the non-relativistic QZP basis set, and then the contraction coefficients of this set were reoptimized using the minimum ZORA-ROHF (restricted open-shell HF) energy criterion. In this process, the digit-by-digit optimization method of nonlinear parameters,[44] which was coupled to the ORCA 4.0 program,[45] was employed. It should be noted that the exponents of the GTFs and the segmented contraction schemes of the original QZP basis set were not altered in this optimization process. For Hf–Hg, it is worth remembering that Pantazis *et al.* also reoptimized only the contraction coefficients of a non-relativistic basis set to generate sets that have been designated as SARC-ZORA.[43]

Table 1. Details regarding the QZP-ZORA and AQZP-ZORA basis sets for H–Xe.

	Set	Uncontracted set	Contracted set
H, He	QZP- ZORA	(6s3p2d1f)	[4s3p2d1f]
	AQZP-ZORA	(7s4p3d2f)	[5s4p3d2f]
Li-Ne	QZP-ZORA	(11s7p3d2f1g)	[6s4p3d2f1g]
	AQZP-ZORA	(12s8p4d3f2g)	[7s5p4d3f2g]
Na–Ar	QZP-ZORA	(14s11p3d2f1g)	[9s6p3d2f1g]
Na	AQZP-ZORA	(15s11p4d3f2g)	[10s6p4d3f2g]
Mg–Ar	AQZP-ZORA	(15s12p4d3f2g)	[10s7p4d3f2g]
K, Ca	QZP-ZORA	(17s14p3d2f1g)	[10s7p3d2f1g]
	AQZP-ZORA	(18s15p4d3f2g)	[11s8p4d3f2g]
Sc–Kr	QZP-ZORA	(17s14p7d3f2g1h)	[10s7p4d3f2g1h]
Sc, Mn–Ni, Zn–Kr	AQZP-ZORA	(18s15p8d4f3g2h)	[11s8p5d4f3g2h]
Ti–Cr, Cu	AQZP-ZORA	(18s14p8d4f3g2h)	[11s7p5d4f3g2h]
Rb, Sr	QZP-ZORA	(21s17p8d2f1g)	[10s8p4d2f1g]
	AQZP-ZORA	(22s18p9d3f2g)	[11s9p5d3f2g]
Y–Nb, Pd	QZP-ZORA	(21s16p10d3f2g1h)	[10s7p5d3f2g1h]
Y	AQZP-ZORA	(22s16p11d4f3g2h)	[11s7p6d4f3g2h]
Zr	AQZP-ZORA	(21s16p11d4f3g2h)	[10s7p6d4f3g2h]
Nb, Pd	AQZP-ZORA	(22s17p11d4f3g2h)	[11s8p6d4f3g2h]
Mo, Tc, Te	QZP-ZORA	(20s17p10d3f2g1h)	[10s8p5d3f2g1h]
Mo, Tc, Te	AQZP- ZORA	(21s18p11d4f3g2h)	[11s9p6d4f3g2h]
Ru, Rh, Ag–Sb, I, Xe	QZP-ZORA	(21s17p10d3f2g1h)	[10s8p5d3f2g1h]
Ru, Rh	AQZP-ZORA	(21s18p11d4f3g2h)	[10s9p6d4f3g2h]
In	AQZP-ZORA	(22s17p11d4f3g2h)	[11s8p6d4f3g2h]
Ag, Cd, Sn, Sb, I, Xe	AQZP-ZORA	(22s18p11d4f3g2h)	[11s9p6d4f3g2h]

To obtain reliable results of some atomic and/or molecular properties, such as electron affinity, polarizability, optical rotation, negative ions, and hydrogen bonds, it is necessary to correctly describe the electrons furthest from atomic nuclei. Diffuse functions of symmetries s, p, d, etc. are added to the basis set. Therefore, to our QZP-ZORA basis set, we add a diffuse function to each atomic symmetry s, p, d, f, g, and h to give rise to the AQZP-ZORA set. These diffuse func-

tions were taken directly from our non-relativistic AQZP basis set.[18,21,22] In Table 1, the sizes of the QZP-ZORA and AQZP-ZORA uncontracted and contracted basis sets of each element from H to Xe are displayed. It may be noted that for some symmetries of some elements it was impossible to add diffuse functions because the QZP-ZORA set already has functions with this characteristic.

3. Results and discussion

All calculations were performed using the ZORA-CCSD(T) method available in the ORCA 4.0 code.[45] Except for polarizability, all electrons were correlated, and the other properties were obtained using the frozen core approximation for electron correlation. Initially, the geometries of the molecules were optimized and then atomization energies and harmonic vibrational frequencies were calculated from these geometries.

3.1. Atomic ionization energy

Table 2 lists the experimental ionization energies[47] as well as those calculated with the DKH2-CCSD(T)/QZP-DKH,[17,28] ZORA-CCSD(T)/QZP-ZORA, and ZORA-CCSD(T)/x2c-QZVPall-2c theoretical procedures.

As is expected, within each row of the periodic table, the lowest and highest ionization energies occur for the alkalines (Li and K) and noble gases (He, Ne, Ar, Kr, and Xe), respectively. In addition, the ionization energies decrease from top to bottom through group 18 due mainly to increased shielding of the nuclei by electrons. It may be noted that for the elements of groups 13–18, in general, the ionization energies grow from left to right through a row. For the 3d and 4d transition elements, except for a few cases, the ionization energies also grow from left to right.

Except for K and Zr, the QZP-DKH ionization energies are very close to the corresponding QZP-ZORA, with the largest difference of 8.4% occurring for Zr. For K, the QZP-ZORA value is in better agreement with the experimental one than the QZP-DKH, while for Zr, the theoretical results are approximately equidistant from the experimental value. This is not the first time (see Refs. [41,43,48]) that the DKH2 method underestimates the experimental value. To improve the ionization energy of K, it is necessary to use higher theory levels (DKH3, DKH4, etc.). However, this type of correction is beyond the purpose of this work.

Overall, the agreement between theoretical and experimental results is good. Proof of this statement is in the low values of the mean absolute deviations (MADs) of the theoretical ionization energies concerning the experimental data, with slight decreases in MADs going from the QZP-DKH set (0.150) to the QZP-ZORA (0.135) and from the QZP-ZORA to the x2c-QZVPall-2c (0.105). The reason why the x2c-QZVPall-2c all-electron set[46] gives the smallest MAD is owing to the fact that it has many more functions than the other two. For example, for the elements Ne, Ar, Kr, and Xe, the numbers of GTFs used to construct the x2c-QZVPall-2c uncontracted set were 77, 108, 163, and 225, respectively, while for the non-contracted QZP-ZORA set these numbers decrease to 70, 85, 144 and 172, respectively. Indeed, this means that the number of two-electron integrals to be calculated with the QZP-ZORA set is smaller than that with the x2c-QZVPall-2c set. Considering the x2c-QZVPall-2c and QZP-ZORA contracted sets, these numbers are equal to 57, 70, 83, and 112 and 56, 65, 101, and 109, respectively. These last numbers indicate that the dimensions of the diagonalizable matrices of the x2c-QZVPall-2c set are greater than those of the QZP-ZORA set. In summary, the computational time to perform an x2c-QZVPall-2c calculation is significantly greater than QZP-ZORA.

Since the QZP-DKH and QZP-ZORA sets are identical in size and the resulting MADs are very close to each other, we decided that a statistical error analysis should be performed. Initially, considering the experimental ionization energy of each atom, the relative absolute error (RAE) through each theoretical model [DKH2-CCSD(T)/QZP-DKH and ZORA-CCSD(T)/QZP-ZORA] was calculated, and histograms were constructed (see Fig. 1). These histograms are normalized and thus the total area under each curve is equal to one, representing an empirical estimate for the density function of the RAEs. Figure 1 shows the density distributions as a function of RAEs and one note that the density distributions are skewed to the right and that the performance of the ZORA-CCSD(T)/QZP-ZORA theoretical model is better than that of the DKH2-CCSD(T)/QZP-DKH procedure, due to the fact that the RAEs calculated with the first model are more concentrated on the left side of the histogram. This finding is not different from that predicted by the MADs.

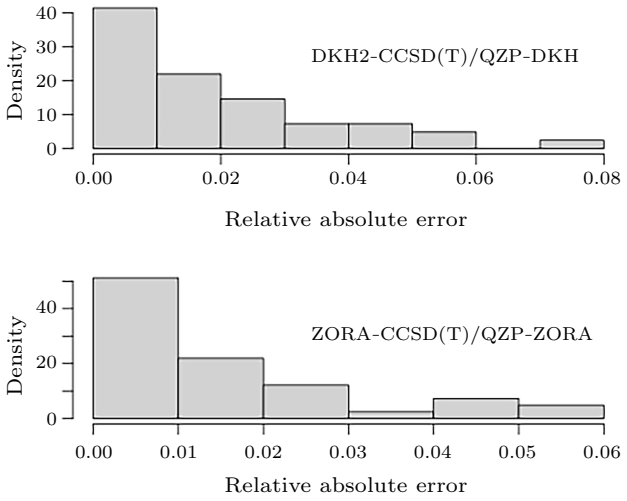


Fig. 1. Histograms of the relative absolute errors for the ionization energies calculated with the DKH2-CCSD(T)/QZP-DKH and ZORA-CCSD(T)/QZP-ZORA theoretical models.

Table 2. Theoretical and experimental ionization energies (in eV) of some elements.

	QZP-DKH[a]	QZP-ZORA[b]	x2c-QZVPall-2c[c]	Expt.[d]
He (^{1}S) → He$^+$ (^{2}S)	24.560	24.562	24.564	24.58739
Li (^{2}S) → Li$^+$ (^{1}S)	5.342	5.349	5.376	5.39171
Be (^{1}S) → Be$^+$ (^{2}S)	9.294	9.233	9.298	9.3227
C (^{3}P) → C$^+$ (^{2}P)	11.201	11.201	11.200	11.2603
N (^{4}S) → N$^+$ (^{3}P)	14.484	14.847	14.486	14.53414
O (^{3}P) → O$^+$ (^{4}S)	13.474	13.475	13.475	13.61806
F (^{2}P) → F$^+$ (^{3}P)	17.296	17.299	17.294	17.42282
Ne(^{1}S) → Ne$^+$ (^{2}P)	21.481	21.473	21.464	21.56454
Mg (^{1}S) → Mg$^+$ (^{2}S)	7.536	7.605	7.615	7.64624
Al (^{2}P) → Al$^+$ (^{1}S)	5.963	5.963	5.960	5.98577
Si (^{3}P) → Si$^+$ (^{2}P)	8.127	8.128	8.126	8.15169
P (^{4}S) → P$^+$ (^{3}P)	10.488	10.491	10.489	10.48669
S (^{3}P) → S$^+$ (^{4}S)	10.216	10.226	10.230	10.36001
Cl (^{2}P) → Cl$^+$ (^{3}P)	12.854	12.859	12.861	12.96764
Ar (^{1}S) → Ar$^+$ (^{2}P)	15.696	15.699	15.701	15.75961
K (^{2}S) → K$^+$ (^{1}S)	4.022	4.325	4.321	4.34066
Ca (^{1}S) → Ca$^+$ (^{2}S)	5.896	6.021	6.086	6.11316
Sc (^{2}D) → Sc$^+$ (^{3}D)	6.389	6.546	6.539	6.56149
Fe (^{5}D) → Fe$^+$ (^{6}D)	7.791	7.596	6.758	7.90247
Ni (^{3}F) → Ni$^+$ (^{2}D)	7.403	7.489	7.624	7.63988
Cu (^{2}S) → Cu$^+$ (^{1}S)	7.555	7.614	7.726	7.72638
Zn (^{1}S) → Zn$^+$ (^{2}S)	9.249	9.297	9.382	9.39420
Ga (^{2}P) → Ga$^+$ (^{1}S)	5.742	5.745	5.933	5.99930
Ge (^{3}P) → Ge$^+$ (^{2}P)	7.763	7.767	7.916	7.89944
As (^{4}S) → As$^+$ (^{3}P)	9.821	9.831	10.005	9.78855
Se (^{3}P) → Se$^+$ (^{4}S)	9.255	9.263	9.552	9.75237
Br (^{2}P) → Br$^+$ (^{3}P)	11.520	11.531	11.784	11.81381
Kr (^{1}S) → Kr$^+$ (^{2}P)	13.960	13.669	14.129	13.99961
Sr (^{1}S) → Sr$^+$ (^{2}S)	5.442	5.630	5.678	5.69487
Zr (^{3}F) → Zr$^+$ (^{4}F)	6.403	6.941	6.564	6.63413
Nb (^{6}D) → Nb$^+$ (^{5}D)	6.805	6.921	6.787	6.75885
Ru (^{5}F) → Ru$^+$ (^{4}F)	7.166	7.369	7.394	7.36050
Rh (^{4}F) → Rh$^+$ (^{3}F)	7.304	7.494	7.490	7.45890
Pd (^{1}S) → Pd$^+$ (^{2}D)	8.336	8.309	8.342	8.33684
Ag (^{2}S) → Ag$^+$ (^{1}S)	7.432	7.582	7.584	7.57623
Cd (^{1}S) → Cd$^+$ (^{2}S)	8.820	8.934	8.985	8.99382
Sn (^{3}P) → Sn$^+$ (^{2}P)	7.193	7.197	7.3081	7.34392
Sb (^{4}S) → Sb$^+$ (^{3}P)	9.022	9.031	9.1162	8.60839
Te (^{3}P) → Te$^+$ (^{4}S)	8.530	8.539	8.689	9.00981
I (^{2}P) → I$^+$ (^{3}P)	10.289	10.305	10.5445	10.45126
Xe (^{1}S) → Xe$^+$ (^{2}P)	12.045	12.068	12.454	12.12984
MAD[e]	0.150	0.135	0.105	–

[a]Refs. [17,28]. The DKH2-CCSD(T) method together with the frozen core approach for electron correlation was used in the calculations. [b]Present investigation. Basis set generated in this work. The ZORA-CCSD(T) method together with the frozen core approach for electron correlation was used in the calculations. [c]Present investigation. Basis set generated in Ref. [46]. The ZORA-CCSD(T) method together with the frozen core approach for electron correlation was used in the calculations. [d]Ref. [47]. [e]Mean absolute deviation from the experimental data.

3.2. Static mean dipole polarizability

It is known that the deformation of the electron cloud due to the presence of an external electric field is related to the mean dipole polarizability and that this property is sensitive to the theoretical approach used to evaluate it. Therefore, it will be a good test for the AQZP basis set.

Table 3 shows the static mean dipole polarizabilities DKH2-CCSD(T)/AQZP-DKH and ZORA-CCSD(T)/AQZP-ZORA. Recommended and experimental values reported in Ref. [49] were also included.

A behavior opposite to that of ionization energies is observed for polarizabilities, i.e., for the elements of columns 13–18 of each row they decrease from left to right. For the 3d and 4d transition metals, a decrease in the mean dipole polarizabilities from left to right can also be noted. Again, this tendency is the exact opposite to that of ionization energies. In summary, the behaviors of ionization energies and mean dipole polarizabilities for the elements studied herein correspond to what is predicted based on chemistry.

The results computed with the AQZP-DKH and AQZP-

ZORA sets are similar, with the largest difference of 5.7% occurring for Ni. Except for a few cases, the theoretical results are within the uncertainty bars of the recommended and/or experimental values. Regarding the recommended values, the MADs obtained with the DKH2-CCSD(T)/AQZP-DKH and ZORA-CCSD(T)/AQZP-ZORA theoretical models are equal to 2.046 a.u. and 1.849 a.u., respectively. Considering the experimental data, these deviations increase to 4.483 a.u. and 4.741 a.u. Considering that some experimental values are not very reliable, the MADs calculated concerning the recommended values are very small, since the mean dipole polarizabilities of several elements exceed 100 a.u., and can reach 320 a.u. Thus, these results indicate that the performance of the AQZP-ZORA basis set appears to be promising in determining the property that depends on an accurate description of electrons distant from the nuclei. Once again, the performances of the DKH2 and ZORA Hamiltonians proved not to be much different.

Table 3. Static mean dipole polarizabilities for the ground states of some elements. All values are in a.u.

Atom	AQZP-DKH[a]	AQZP-ZORA[b]	Recommended value[c]	Expt.[d]
He	1.35397	1.35382	1.38375 ± 0.00002	1.383746 ± 0.000007
Be	37.958	38.390	37.74 ± 0.03	37.8
C	11.553	11.491	11.3 ± 0.2	11.87708
N	7.249	7.227	7.4 ± 0.2	7.6 ± 0.4
O	5.153	5.157	5.3 ± 0.2	5.2 ± 0.4
Mg	72.256	75.155	71.2 ± 0.4	71.5 ± 3.5
Al	58.855	58.280	57.8 ± 1.0	55.3 ± 5.5
P	25.106	25.123	25 ± 1	24.49648
Cl	14.617	15.127	14.6 ± 0.1	14.71139
K	291.735	288.370	289.7 ± 0.3	292.9 ± 6.1
Ca	163.500	164.247	160.8 ± 4.0	169 ± 17
V	85.071	88.925	87 ± 10	68.2 ± 5.4
Cr	82.921	82.812	83 ± 10	60 ± 24
Ni	50.763	48.026	49 ± 3	–
Zn	37.199	37.176	38.67 ± 0.30	38.8 ± 0.8
Ga	51.336	50.969	50 ± 3	46.6 ± 4.0
Ge	39.852	39.670	40 ± 1	–
As	29.505	29.435	30 ± 1	–
Br	20.477	20.711	21 ± 1	20.58244
Kr	16.506	16.648	16.78 ± 0.02	16.766 ± 0.008
Rb	326.574	323.619	319.8 ± 0.3	319.2 ± 6.1
Sr	206.616	205.094	197.2 ± 0.2	186 ± 15
Nb	104.741	104.897	98 ± 8	97.9 ± 7.4
Mo	84.504	83.848	87 ± 6	87.1 ± 6.1
Rh	57.824	59.494	66 ± 10	–
Ag	49.738	49.582	55 ± 8	45.9 ± 7.4
Cd	44.986	44.910	46 ± 2	45.3 ± 1.4
In	67.305	66.089	65 ± 4	62.1 ± 6.1
Sn	58.145	55.577	53 ± 6	67.5 ± 8.8
Sb	42.605	42.427	43 ± 2	–
Te	37.370	37.113	38 ± 4	–
I	31.563	31.534	32.9 ± 1.3	32.9 ± 1.3
MAD[e]	2.046	1.849	–	–
MAD[f]	4.483	4.741	–	–

[a]Present investigation. Basis set generated in Refs. [18,21,22]. The full DKH2-CCSD(T) method was used in the calculations. [b]Present investigation. Basis set generated in this work. The full ZORA-CCSD(T) method was used in the calculations. [c]Ref. [49]. [d]Taken from Ref. [49]. [e]Mean absolute deviation from the recommended values. [f]Mean absolute deviation from the experimental data.

3.3. Bond length

Table 4 presents geometric parameters, atomization energies, and harmonic vibrational frequencies of some molecules in the ground states computed with the QZP-DKH and QZP-ZORA basis sets. As a benchmark, experimental data[50,51] were also included.

For SO_2, the bond angles obtained with the DKH2-CCSD(T)/QZP-DKH and ZORA-CCSD(T)/QZP-ZORA procedures lead to similar results and in excellent agreement with the experimental data. The previous theoretical models as well as the experiments show an increase in bond lengths going from KF to RbF, from As_2 to Sb_2, from SnSe to SnTe, and from IF to ICl. This was already expected due to the increase in atomic radii along the columns of alkali metals, pnictogens, chalcogens, and halogens. Also notably, the main reason why the bond length of CuH is shorter than that of ZnH is that the 4s orbitals of Cu and Zn have 1 and 2 electrons, respectively.

Table 4. Theoretical and experimental bond lengths (r_e in Å), atomization energies (D_0 in kcal/mol), and harmonic vibrational frequencies (ω_e in cm^{-1}) of some molecules in the ground states.

		QZP-DKH[a]	QZP-ZORA[b]	Expt.[c]
CO_2 ($^1\Sigma_g^+$)	r_e	1.1623	1.1623	1.1600
	D_0	375.684	374.505	381.752
	ω_e	670.45	668.68	672
		1351.27	1350.43	1351
		2394.64	2392.99	2396
SO_2 ($^1A_1$)	r_e	1.4439	1.4435	1.4308
	θ_e	118.608	118.623	119.329
	D_0	239.101	238.832	249.484
	ω_e	524.73	537.88	526
		1172.66	1169.22	1168
		1384.27	1357.28	1381
KF ($^1\Sigma^+$)	r_e	2.2681	2.1681	2.1715
	D_0	111.257	111.506	118.9 ± 0.6
	ω_e	415.34	426.26	433.23
CuH ($^1\Sigma^+$)	r_e	1.4470	1.4411	1.4626
	D_0	62.369	63.103	62.955
	ω_e	1969.96	1993.55	1940.77
Cu_2 ($^1\Sigma_g^+$)	r_e	2.2266	2.2161	2.2197
	D_0	43.803	44.498	46.813
	ω_e	260.96	263.97	264.55
ZnH ($^2\Sigma^+$)	r_e	1.5813	1.5733	1.5949
	D_0	20.076	20.083	20.5 ± 0.5
	ω_e	1634.6	1661.81	1607.6
GaCl ($^1\Sigma^+$)	r_e	2.2061	2.2039	2.2017
	D_0	112	112.019	114 ± 3
	ω_e	366.28	364.23	365.67
Ga_2 ($^3\Pi_u$)	r_e	2.6519	2.6518	–
	D_0	27.593	27.587	26.4 ± 1.7
	ω_e	174.8	172.72	178.2
Ge_2 ($^3\Sigma_g^-$)	r_e	2.4099	2.4078	2.3689
	D_0	62.357	62.204	62.3 ± 1.7
	ω_e	283.9	285.58	287.91
As_2 ($^1\Sigma_g^+$)	r_e	2.1242	2.1219	2.103
	D_0	79.450	79.265	90.557
	ω_e	424.4	423.44	429.6
Se_2 ($^3\Sigma_g^-$)	r_e	2.1660	2.1642	2.1662
	D_0	80.777	80.486	78.6
	ω_e	405.5	406.98	386.6
BrO ($^2\Pi$)	r_e	1.7146	1.7156	1.7172
	D_0	58.389	58.055	55.2 ± 0.4
	ω_e	710.2	682.54	732.9
Br_2 ($^1\Sigma_g^+$)	r_e	2.2680	2.2660	2.2810
	D_0	51.162	50.923	45.44
	ω_e	344.9	342.60	325.3
RbF ($^1\Sigma^+$)	r_e	2.4121	2.2702	2.27033
	D_0	111.574	112.477	115.3
	ω_e	366.38	373.84	376
SrH ($^2\Sigma^+$)	r_e	2.237	2.1787	2.1456
	D_0	38.097	35.624	$\leqslant 38.3$
	ω_e	1172.14	1167.54	1206.2
ZrO ($^1\Sigma^+$)	r_e	1.7411	1.7145	1.7116
	D_0	177.294	182.431	181
	ω_e	950.55	984.55	969.8
InCl ($^1\Sigma^+$)	r_e	2.4065	2.4063	2.4012
	D_0	106.445	106.442	102.389
	ω_e	317.03	313.56	317.39
In_2 ($^3\Pi_u$)	r_e	2.984	3.0042	–
	D_0	25.227	25.053	23.291
	ω_e	121.44	121.31	–
SnSe ($^1\Sigma^+$)	r_e	2.3090	2.3048	2.326
	D_0	108.449	108.361	95.890 ± 1.4
	ω_e	326.36	327.79	331.2
SnTe ($^1\Sigma^+$)	r_e	2.4990	2.4927	2.52280
	D_0	99.909	100.067	85.994
	ω_e	257.27	258.73	259.5
Sb_2 ($^1\Sigma_u^+$)	r_e	2.4961	2.4906	2.476
	D_0	64.856	64.896	69.065
	ω_e	276.41	276.11	269.62
IF ($^1\Sigma^+$)	r_e	1.8967	1.8965	1.9098
	D_0	70.259	69.877	65.3 ± 0.9
	ω_e	640.89	640.13	610.24
ICl ($^1\Sigma^+$)	r_e	2.3023	2.3015	2.3209
	D_0	57.927	57.728	49.64 ± 0.03
	ω_e	409.21	406.21	384.29
MAD[d]	r_e	0.0282	0.0135	–
MAPE[e]	D_0	6.049	6.024	–
	ω_e	2.01	2.18	–

[a]Refs. [17,28]. The DKH2-CCSD(T) method together with the frozen core approach for electron correlation was used in the calculations. [b]Present investigation. Basis set generated in this work. The ZORA-CCSD(T) method together with the frozen core approach for electron correlation was used in the calculations. [c]Refs. [50,51]. [d]Mean absolute deviation from the experimental data. [e]Mean absolute percentage error from the experimental data.

Except for molecules containing alkali metals and alkaline earth metals, the prediction of the bond lengths of all the others is similar. For KF, RbF, and SrH, the QZP-ZORA results are closer to the experimental values than the QZP-DKH and should be decisive in the calculations of deviations. It is worth noting that to improve the bond lengths of these three molecules, it is necessary to use relativistic corrections of higher orders (DKH3, DKH4, etc.). Overall, the MADs of the DKH2-CCSD(T)/QZP-DKH and ZORA-CCSD(T)/QZP-ZORA theoretical models concerning the experimental data are 0.0282 Å and 0.0135 Å, respectively. The latter value is less than half of the former and its reduced magnitude shows the excellent performance of the ZORA approximation in determining bond lengths. Due to this difference between MADs, we decided to perform a statistical error analysis again. The RAEs of the DKH2-CCSD(T)/QZP-DKH and ZORA-CCSD(T)/QZP-ZORA bond lengths relative to the experimental data were calculated and histograms of these errors were then constructed (see Fig. 2). The histograms were normalized so that their total areas were equal to one. Again, the curves resulting from the densities as a function of the RAEs show distributions skewed to the right. In addition, since the RAEs obtained from the ZORA-CCSD(T)/QZP-ZORA procedure are closer to the origin of the coordinate system than those computed with DKH2-CCSD(T)/QZP-DKH, this shows a better performance of the first model. This is in line with the prediction made through the MADs.

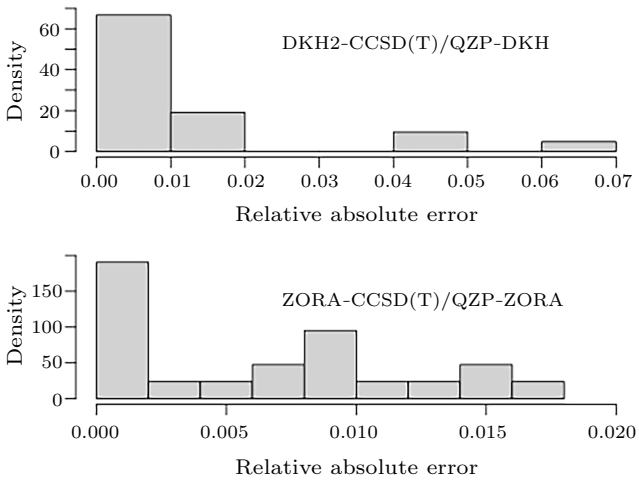


Fig. 2. Histograms of the relative absolute errors for the bond lengths calculated with the DKH2-CCSD(T)/QZP-DKH and ZORA-CCSD(T)/QZP-ZORA theoretical models.

3.4. Atomization energy

Our findings reveal that there is an increase in the bond lengths from As_2 to Sb_2, from SnSe to SnTe, and from IF to ICl, meanwhile, the dissociation energies decrease. The relationship between bond lengths and dissociation energies has already been extensively explored in the literature (see, e.g., Ref. [52]). The dissociation energy from CuH to ZnH de-

creases due to the increase in bond length and the number of electrons in the 4s orbital.

Except for the SrH and ZrO molecules, one notes that the calculated atomization energies are very close to each other. For the SrH molecule, the dissociation energies obtained from the QZP-DKH theoretical model and the experiment are practically identical, while for ZrO, the QZP-ZORA dissociation energy is closer to the experimental value. From these observations, it is expected that the deviation magnitudes obtained based on theoretical procedures will not be very different. Overall, the mean absolute percent errors (MAPEs) of the DKH2-CCSD(T)/QZP-DKH (6.049%) and ZORA-CCSD(T)/QZP-ZORA (6.024%) make the experimental data confirm our qualitative prediction made earlier, with a slight advantage for the ZORA Hamiltonian. To reduce these MAPEs, it is necessary to consider mainly the SO couplings, which are not negligible for some molecules studied in this work.

3.5. Harmonic vibrational frequency

The harmonic vibrational frequency decreases from KF to RbF due to increases in bond length and molecular weight. Similar reasons explain the decreases in harmonic vibrational frequencies going from As_2 to Sb_2, from SnSe to SnTe, and from IF to ICl. From CuH to ZnH, the dominant factor associated with a significant decrease of 20.5% in harmonic vibrational frequency is a 9.3% increase in bond length, while molecular weight increases only 2.9%.

The harmonic vibrational frequencies computed with the two theoretical models are very close to each other, with the largest difference of 4.1% occurring for BrO. A more detailed analysis shows that, in general, the QZP-ZORA results are farther from the experimental data than the QZP-DKH. Therefore, it is expected that the deviations will not be much different and that the one obtained from the QZP-DKH set will be slightly smaller. Overall, considering the experimental data, the MAPEs obtained with the DKH2-CCSD(T)/QZP-DKH and ZORA-CCSD(T)/QZP-ZORA procedures are 2.01% and 2.18%, respectively.

Although the ZORA results presented in this article are, in general, slightly closer to the experimental values than the DKH2, it is hasty to state that the ZORA Hamiltonian is more accurate than the DKH2, since these Hamiltonians only consider the scalar relativistic correction. It is known that there is a lot of "missing physics" in these calculations when compared to experiments, namely, core correlation effects, higher order correlation, SO coupling, and so on. Furthermore, it would be necessary to study a much larger number of molecules. This means that it is difficult to know whether, for example, the ZORA correction is systematically too large and exceeds the true extent of a relativistic correction. In any case, answering the question of which of these two Hamiltonians is the best, considering the desired precision, is certainly outside the scope of this investigation.

3.6. Core-valence correction and spin–orbit coupling

The basis sets generated in this work are highly accurate in atomic and molecular property calculations. To improve the agreement between the properties obtained from theory and experiment, we added to the QZP-ZORA spectroscopic results the SO couplings and/or the core-valence (CV) electron correlation found in the literature.

For InCl, In_2, and Sb_2, the atomic SO coupling corrections were extracted from the experimental dissociation energies.[50–53] Comparing the values resulting from this operation (109 ± 2, 26.169, and 69.032 kcal/mol) with the QZP-ZORA (106.442, 25.053, and 64.896 kcal/mol) listed in Table 4, a significant improvement in the agreement between theory and experiment can be observed. For IF and ICl molecules, adding the ZORA-CCSD(T)/QZP-ZORA dissociation energies (see Table 4) the SO couplings and the CV corrections, estimated in Ref. [54], we found 64.177 kcal/mol and 51.828 kcal/mol, respectively. These results are in good agreement with the experimental values for IF (65.3 ± 0.9) and ICl (49.64 ± 0.03) molecules.[51] For BrO molecule, the SO couplings and CV corrections on r_e, D_0, and ω_e were reported in Ref. [55]. Regarding these corrections in the ZORA-CCSD(T)/QZP-ZORA calculations, we found $r_e = 1.7087$ Å, $D_0 = 55.955$ kcal/mol, and $\omega_e = 690.84$ cm^{-1}, which agree very well with the experimental data of 1.7172 Å, (55.2 ± 0.4) kcal/mol, and 732.9 cm^{-1}, respectively.

Table 5 shows the bond lengths, dissociation energies, and harmonic vibrational frequencies obtained by QZP-ZORA and QZP-ZORA + CV for some molecules, as well as experimental data. The CV corrections were taken from Refs. [39, 56], whereas for Ga_2, Ge_2, Se_2, and Br_2 molecules, SO coupling corrections were extracted from the experimental dissociation energies.[50,51,57,58]

Regarding the QZP-ZORA results with the inclusion of the CV corrections and experimental data, one notes a better corroboration between them. The agreement between the QZP-ZORA + CV dissociation energies and experimental data without SO corrections is very good. For CuH, Ga_2, and Br_2 molecules, these dissociation energies are almost the same. For Ge_2, considering the uncertainty bars of the experimental dissociation energy, the agreement with the QZP-ZORA + CV result is good. The accuracies achieved with the QZP-ZORA + CV approximation for the bond lengths of Cu_2, Ge_2, and As_2 and the harmonic vibrational frequencies of Cu_2, Ga_2, Ge_2, and As_2 are impressive, since they are very close to

the experimental values. The dissociation energy of the arsenic dimer was calculated without SO corrections on the atom and molecule. For As_2, Table 5 shows that the inclusion of CV correction improves the agreement between theory and experiment, but is still not sufficient to produce a satisfactory energy value. To overcome this problem, it is necessary to use larger basis sets,[55] or to use a full potential curve[36] for the ground state of that molecule.

Table 5. Theoretical and experimental bond lengths (r_e in Å), dissociation energies (D_0 in kcal/mol), and harmonic vibrational frequencies (ω_e in cm^{-1}) of some molecules in the ground states.

		QZP-ZORA[a]	QZP-ZORA + CV[b]	Expt.[c]
CuH ($^1\Sigma^+$)	r_e	1.4411	1.4425	1.4626
	D_0	63.103	62.773	62.955
	ω_e	1993.55	1.990.05	1940.77
Cu_2 ($^1\Sigma_g^+$)	r_e	2.2161	2.2163	2.2197
	D_0	44.498	44.248	46.813
	ω_e	263.97	264.47	264.55
Ga_2 ($^3\Pi_u$)	r_e	2.6518	2.5784	–
	D_0	27.587	28.787	(28.391 ± 1.697)[d]
	ω_e	172.72	178.92	178.2
Ge_2 ($^3\Sigma_g^-$)	r_e	2.4078	2.3716	2.3689
	D_0	62.204	63.704	(67.667 ± 1.697)[d]
	ω_e	285.58	291.78	287.9l
As_2 ($^1\Sigma_g^+$)	r_e	2.1219	2.0982	2.103
	D_0	79.265	81.565	90.557
	ω_e	423.44	432.94	429.6
Se_2 ($^3\Sigma_g^-$)	r_e	2.1642	2.1484	2.1662
	D_0	80.486	81.486	(83.960)[d]
	ω_e	406.98	411.78	386.6
Br_2 ($^1\Sigma_g^+$)	r_e	2.2660	2.2533	2.2810
	D_0	50.923	51.123	(52.376)[d]
	ω_e	342.60	346.00	325.3

[a]Present investigation. Basis set generated in this work. The ZORA-CCSD(T) method together with the frozen core approach for electron correlation was used in the calculations. [b]The core-valence corrections were taken from the Refs. [39,56]. [c]Refs. [50,51]. [d]In parentheses are the experimental dissociation energies without SO corrections.[43,44,52,59]

4. Conclusions

The QZP-ZORA basis set for the elements from H to Xe developed herein, together with the DZP-ZORA[43] and TZP-ZORA,[41] forms a hierarchical sequence of basis sets of increasing size. The main goal of this family is to reduce the truncation error of basis sets. It was augmented with diffuse functions, giving rise to the set designated as AQZP-ZORA, to describe electrons distant from atomic nuclei appropriately. Even though these basis sets have quadruple zeta valence quality, they are compact enough to be applied to medium-sized molecules. In addition, their number of primitive functions is smaller than that of any other set of similar quality published in the literature. Recall that the number of primitive functions is associated with the number of two-electron integrals to be calculated. The applications carried out in this work confirm the good performance of both sets.

The following are some specific conclusions associated with the results of this study.

(1) Regarding the experimental ionization energies, the MAD of 0.135 eV shows the excellent performance of the ZORA-CCSD(T)/QZP-ZORA procedure and it is slightly lower than that obtained with the DKH2-CCSD(T)/QZP-DKH model.

(2) Bearing in mind that the mean dipole polarizabilities of various elements are greater than 100 a.u. and can reach 300 a.u., the MAD AQZP-ZORA of 1.849 a.u., relative to the recommended values,[49] is small and again lower than the AQZP-DKH.

(3) The agreements between the bond lengths and harmonic vibrational frequencies QZP-ZORA and the experimental values are good, since the MAD and MAPE are only 0.0132 Å and 2.18%, respectively. As for the atomization energies, the agreement is satisfactory, considering that the MAPE is 6.024%. The main reason for this value is due to the neglect of the SO couplings of some molecules. Except for the bond lengths, where the MAD QZP-DKH is approximately twice that of the QZP-ZORA, the performance of the two basis sets for the other spectroscopic properties is about the same.

(4) For InCl, In_2, Sb_2, IF, ICl, and BrO, it has been shown that when SO couplings are somehow taken into account, the agreement between the ZORA-CCSD(T)/QZP-ZORA and experimental dissociation energies improves significantly.

(5) It can be seen that a high level of accuracy is achieved

when CV corrections are added to the QZP-ZORA results and the SO couplings are removed from the experimental dissociation energies. Various values of bond lengths, dissociation energies, and harmonic vibrational frequencies QZP-ZORA + CV practically coincide with the experimental data.

This work clearly showed that when the necessary corrections are added to results obtained with an accurate theoretical model and/or to experimental data, i.e., the closer we get to the actual description of an electron system, there will always be an improvement in the agreement between theoretical and experimental values.

All parameters of the QZP-ZORA and AQZP-ZORA sets are available on the following website https://qcgv.ufes.br

Acknowledgment

We would like to acknowledge the financial support of Conselho Nacional de Desenvolvimento Científico e Tecnológico and Coordenação de Aperfeiçoamento de Pessoal de Nível Superior (Brazilian Agencies).

References

[1] Schäfer A, Horn H and Ahlrichs R 1992 *J. Chem. Phys.* **97** 2571
[2] Schäfer A, Huber C and Ahlrichs R 1994 *J. Chem. Phys.* **100** 5829
[3] Weigend F, Furche F and Ahlrichs R 2003 *J. Chem. Phys.* **119** 12753
[4] Almlöf J and Taylor P R 1987 *J. Chem. Phys.* **86** 4070
[5] Dunning Jr T H 1989 *J. Chem. Phys.* **90** 1007
[6] Woon D E and Dunning Jr T H 1993 *J. Chem. Phys.* **98** 1358
[7] Wilson A K, van Mourik T and Dunning Jr T H 1996 *J. Mol. Struct. THEOCHEM* **388** 339
[8] Wilson A K, Woon D E, Peterson K A and Dunning Jr T H 1999 *J. Chem. Phys.* **110** 7667
[9] Raffenet R C 1973 *J. Chem. Phys.* **58** 4452
[10] Dunning Jr T H 1970 *J. Chem. Phys.* **53** 2823
[11] Canal Neto A, Muniz E P, Centoducatte R and Jorge F E 2005 *J. Mol. Struct. THEOCHEM* **718** 219
[12] Camiletti G G, Machado S F and Jorge F E 2008 *J. Comp. Chem.* **29** 2434
[13] Barros C L, de Oliveira P J P, Jorge F E, Canal Neto A and Campos M 2010 *Mol. Phys.* **108** 1965
[14] Barbieri P L, Fantin P A and Jorge F E 2006 *Mol. Phys.* **104** 2945
[15] Machado S F, Camiletti G G, Canal Neto A, Jorge F E and Jorge R S 2009 *Mol. Phys.* **107** 1713
[16] Campos C T and Jorge F E 2013 *Mol. Phys.* **111** 167
[17] Ceolin G A, de Berrêdo R C and Jorge F E 2013 *Theor. Chem. Acc.* **132** 1339
[18] Ferreira I B, Campos C T and Jorge F E 2020 *J. Mol. Model.* **26** 95
[19] Camiletti G G, Canal Neto A, Jorge F E and Machado S F 2009 *J. Mol. Struct. THEOCHEM* **910** 122
[20] De Oliveira P J P, Barros C L, Jorge F E, Canal Neto A and Campos M 2010 *J. Mol. Struct. THEOCHEM* **948** 43
[21] Fantin P A, Barbieri P L, Canal Neto A and Jorge F E 2007 *J. Mol. Struct. THEOCHEM* **810** 103
[22] Martins L S C, de Souza F A L, Ceolin G A, Jorge F E, de Berrêdo R C and Campos C T 2013 *Comput. Theor. Chem.* **1013** 62
[23] Van Lenthe E, Baerends E J and Snijders J G 1993 *J. Chem. Phys.* **99** 4597
[24] Douglas M and Kroll N M 1974 *Ann. Phys.* **82** 89
[25] Hess B A 1985 *Phys. Rev. A* **32** 756
[26] Hess B A 1986 *Phys. Rev. A* **33** 3742
[27] De Jong W A, Harrison R J and Dixon D A 2001 *J. Chem. Phys.* **114** 48
[28] Jorge F E, Canal Neto A, Camiletti G G and Machado S F 2009 *J. Chem. Phys.* **130** 064108
[29] De Almeida C A, Pinto L P N M, dos Santos H F and Paschoal D F S 2021 *J. Mol. Model.* **27** 322
[30] Mikherdov A S, Jin M and Ito H 2023 *Chem. Sci.* **14** 4485
[31] Lavrenova L G, Ivanova A I, Glinskaya L A, Artem'ev A V, Lavrov A N, Novikov A S and Abramov P A 2023 *Chem. Asian J.* **18** e202201200
[32] Fomenko I S, Koshcheeva O S, Kuznetsova N I, Larina T V, Gongola M I, Afewerki M, Abramov P A, Novikov A S and Gushchin A L 2023 *Catalysts* **13** 849
[33] Jorge F E and de Macedo L G M 2016 *Chin. Phys. B* **25** 123102
[34] Jorge F E and Venancio J R C 2018 *Chin. Phys. B* **27** 063102
[35] Roos B O, Lindh R, Malmqvist P Å, Veryazov V and Widmark P O 2005 *J. Phys. Chem. A* **109** 6575
[36] Roos B O, Lindh R, Malmqvist P Å, Veryazov V and Widmark P O 2004 *J. Phys. Chem. A* **108** 2851
[37] Roos B O, Veryazov V and Widmark P O 2004 *Theor. Chem. Acc.* **111** 345
[38] Noro T, Sekiya M and Koga T 2012 *Theor. Chem. Acc.* **131** 1124
[39] Balabanov N B and Peterson K A 2005 *J. Chem. Phys.* **123** 064107
[40] Peterson K A, Figgen D, Dolg M and Stoll H 2007 *J. Chem. Phys.* **126** 124101
[41] Canal Neto A, Ferreira I B, Jorge F E and de Oliveira A Z 2021 *Chem. Phys. Lett.* **771** 138548
[42] Pantazis D A, Chen X Y, Landis C R and Neese F 2008 *J. Chem. Theory Comput.* **4** 908
[43] Canal Neto A, de Oliveira A Z, Jorge F E and Camiletti G G 2021 *J. Mol. Model.* **27** 232
[44] Jorge F E and Canal Neto A 2020 *Theor. Chem. Acc.* **139** 76
[45] Neese F 2018 *WIREs Comput. Mol. Sci.* **8** e1327
[46] Franzk Y J, Spiske L, Pollak P and Weigend F 2020 *J. Chem. Theory Comput.* **16** 5658
[47] Kramida A, Ralchenko Yu, Reader J and NIST ASD Team 2023 NIST Atomic Spectra Database (ver. 5.11)
[48] Centoducatte R, de Oliveira A Z, Jorge F E and Camiletti G G 2022 *Comput. Theor. Chem.* **1207** 113511
[49] Schwerdtfeger P and Nagle J K 2019 *Mol. Phys.* **117** 1200
[50] Lide D R (Ed.) 2003-2004 *CRC Handbook of Chemistry and Physics* 84th edn (CRC Press)
[51] Huber K P and Herzberg G 1979 *Molecular Spectra and Molecular Structure. IV. Constants of Diatomic Molecules* (New York: Van Nostrand Reinhold)
[52] Sontag H and Weber R 1982 *J. Mol. Spectrosc.* **91** 72
[53] Chase Jr M W 1998 *J. Phys. Chem. Ref. Data Monograph* vol. 9. *NIST-JANAF Thermochemical Tables*, 4th edn, Part I, Al–Co (New York: American Institute of Physics)
[54] Feller D, Peterson K A, de Jong W A and Dixon D A 2003 *J. Chem. Phys.* **118** 3510
[55] Peterson K A, Shepler B C, Figgen D and Stoll H 2006 *J. Phys. Chem. A* **110** 13877
[56] DeYonker N J, Peterson K A and Wilson A K 2007 *J. Phys. Chem. A* **111** 11383
[57] Shim I, Mandix K and Gingerich K A 1991 *J. Phys. Chem.* **95** 5435
[58] Kingcade J E, Nagarathna-Naik H M, Shim I and Gingerich K A 1986 *J. Phys. Chem.* **90** 2830
[59] Zavitsas A A 2003 *J. Phys. Chem. A* **107** 897